

Numerical Investigation of the Influence of Fin Contraction on Heat Transfer in Fe₃O₄ - SiC - Al₂O₃ / Silicone Oil Ternary Hybrid Nanofluid

Ammembaal Gopalkrishna Pai, Rekha G. Pai and Karthi Pradeep

Abstract—This study numerically investigates the variation in the fin structure on the thermal performance of an axially aligned porous fin embedded in ternary hybrid nanofluid. The tapered wet porous fin moving at a uniform speed is subjected to expansion and contraction. The thermal performance of the embedded model is numerically evaluated through simulation based on the impact of this on the fin's temperature distribution and temperature gradient. The study employs a systematic approach by non-dimensionalizing the governing equation and obtaining the numerical solution using Lobatto numerical technique. Darcy's flow model is applied to examine the proposed model key parameters and thermal characteristics of ternary hybrid nanofluid within the fin, accounting for natural convection and radiation effects. The simulation results highlight the implication of various similarity parameters and variation in the fin profile on the thermal behaviour of the embedded model. A substantial enhancement in the heat transmission is observed, attributed to fin contraction. Statistically, the heat absorption by the surrounding ternary hybrid nanofluid enhances by an average of 1.82%, 1.76%, 1.82%, 3.39% with the enhancement in the similarity parameters NC , n_2 , NR , PE values and 1.91%, 1.96% with the decrease in the similarity parameters q , θ_{a1} , as the fin contracts along its length. Also, the temperature gradient enhances with the fin contraction. The findings enhance the understanding of fin design, hybrid nanofluid flow and its potential applications in the design and optimization of thermal management systems in industries. Additionally, they lay the foundation for carrying out further research in hybrid nanofluid based cooling systems.

Index Terms—Ternary Hybrid Nanofluid, Fin, Thermal Conductivity, Contraction, Heat Transfer.

NOMENCLATURE

Symbol	Quantity
L_1	Length of the fin (m)
\dot{m}	Mass flow rate of the fluid
Q	Heat transfer rate
v	Passage velocity
ϑ	Effective kinematic viscosity (m ² /s)
C_p	Specific heat with constant pressure (J/kgK)
T	Local fin surface temperature (K)
K_1	Permeability (N/A ²)

Symbol	Quantity
T_A	Surrounding ternary hybrid nano fluid temperature (K)
T_B	Prime surface temperature (K)
x_1	Axial distance (m)
\hat{S}	Stretching/shrinking parameter of the fin (1/m)
S_1	Dimensionless stretching/shrinking parameter
A	Fin taper ratio
q	Exponential index
n_1, n_0	Constants
NC	Convection parameter
NR	Radiation parameter
n_2	Wet porous parameter
g_1	Acceleration due to gravity (m/s ²)
h_1	Heat transfer coefficient (W/m ² K)
h_{a1}	Convective heat transfer coefficient at T_A
i_{fg}	Latent heat of water evaporation (J/Kg)
W_1	Width of the fin
h_{D1}	Uniform mass transfer coefficient
U_1	Constant velocity of the fin (m/s)
Le	Lewis Number
X	The dimensionless axial distance
b_2	Variable parameter
PE	Peclet Number
k	Thermal conductivity (W/mK)
f	Base fluid
nf	Nanofluid
hnf	Hybrid nanofluid
$thnf$	Ternary hybrid nanofluid
$A_1(x_1)$	Fin cross-sectional perimeter as a function of x_1 (m)
$A_c(x_1)$	Fin cross-sectional area as a function of x_1 (m ²)
p_1, p_2, p_3	Nanoparticle 1 (Fe ₃ O ₄), solid nanoparticle 2 (SiC), solid nanoparticle 3 (Al ₂ O ₃)
$\varphi_1, \varphi_2, \varphi_3$	Volume fraction of Fe ₃ O ₄ , SiC, and Al ₂ O ₃ , respectively
σ_1	Stefan-Boltzmann constant (W/m ² K ⁴)
ϕ_1	Porosity
a_1	Empirical constant
α_1	Shape factor
β	Volumetric coefficient of thermal expansion (1/K)
$\hat{\omega}$	Humidity ratio of the saturated air
$\hat{\omega}_a$	Humidity ratio of the surrounding air
ρ_1	Effective density (Kg/m ³)
ε_1	Surface emissivity of fin
μ	Dynamic viscosity
Θ_1	The dimensionless temperature
Θ_{1a}	Ambient non-dimensional temperature
δ_1	Deviation in fin tip (m)

Manuscript received February 17, 2025; revised June 12, 2025

Ammembaal Gopalkrishna Pai is an Assistant Professor in the Department of Electronics and Communication, Manipal Institute of Technology, Manipal Academy of Higher Education, Manipal, Karnataka, 576104 India e-mail: (gopalkrishna.pai@manipal.edu)

Rekha G.Pai is an Associate Professor in the Department of Mathematics, Manipal Institute of Technology, Manipal Academy of Higher Education, Manipal, Karnataka, 576104 India (corresponding author to provide phone: +91-8310480979; e-mail: pai.rekha@manipal.edu)

Karthi Pradeep is an Assistant Professor in the Department of Electronics and Communication, Manipal Institute of Technology, Manipal Academy of Higher Education, Manipal, Karnataka, 576104 India e-mail: (karthi.pradeep@manipal.edu).

I. INTRODUCTION

NANOMATERIAL science has transformed the area of thermal management system, unlocking the innovative approaches to enhance the thermal performance across diverse engineering application, from power electronics to

aerospace design. Effective heat transfer is crucial for driving technological advancements, such as the optimization of energy systems and miniaturization of electronics. Recently, researchers have explored a wide range of solutions to address these challenges. One of the commonly used techniques in Industries involves application of fluids over different geometries. Benkhedda et al. [1] numerically investigated the heat transfer and hydrodynamic behaviour of a hybrid nanofluid with a varying volume fraction ranging from 0 to 8%, flowing through an isothermally heated cylindrical tube. Enhancing the flow dynamics and heat transmission efficiency in transformer cooling systems using various fin geometries were analysed through simulation by Farhan et al. [2]. The simulation results indicated a notable drop in temperature with the conic-shaped fins. Ma et al. [3] conducted research on phase change materials using various fin geometries to improve the thermal performance of the LHTES system. Rectangular fins showed an exceptional performance in heat transmission over the rest of the shapes. An in-depth analysis of heat sinks with various fin arrangements and geometries was carried out by Gaikwad et al. [4]. Sharma et al. [5] experimentally investigated the heat transfer coefficient and critical heat flux of hybrid nanofluids using silver and zinc oxide nanoparticles. Their findings revealed an enhancement in these parameters with the rise in the concentration of nanoparticles. The examination carried out by Dhumal et al. [6] delves into the thermal management of electronic devices by comparing various cooling techniques and methods for effective heat dissipation. It also examines and explores optimization strategies to determine the ideal size and placement of heat sources mounted on a substrate board with an aim to enhance the overall thermal performance. Kannan et al. [7] numerically investigated the heat transmission in rectangular fins with various perforations. The study conducted by Abdulateef et al. [8] showed an enhancement in the heat transmission using a rectangular fin along the boundary of a cylindrical PCM structure. Khudhur et al. [9] explored the advantages of using various fin geometries combined with rectangular parallel fins. The simulation results, along with experimental verification, showed an increase of 38% in the heat transfer coefficient for straight fins combined with semicircular fins compared to straight fins with other geometries. Kundu and Wongwises [10] analysed the thermal performance of fins' primary surface heated with hybrid nanofluid under mixed convection and radiation heat transmission using the decomposition method, with emphasis on the critical role of mixed convection in enhancing heat transmission. The results showcased the Significant potential use of hybrid nanofluids in improving the heat transfer efficiency has been demonstrated. Kiwan and Al-Nimr pioneered the concept of porous fin in their research, demonstrating the application of Darcy's model in the fin design to enhance the thermal performance.

Ramesh et al. [11] examined the thermal efficiency of semi-spherical porous fin using the RKF 45 numerical technique. Asadian et al. [12] investigated the impact of Darcy's and Rayleigh's number on the thermal profile in Si_3N_4 porous rectangular fin using Galerkin's method. The outcome showed an increase in the fin temperature with an increase in the rate of heat generation. Darvishi et al. [13] analysed the effect of various parameters such as porosity,

radiation, and temperature ratio in porous fin on thermal profile using the homotopy analysis method. The result indicates an enhancement in heat transfer due to radiation.

A comprehensive graphical and statistical analysis was performed by Khan et al. [14] to analyse the variation of the inclination angle of fins with various profiles on its heat distribution. The outcome indicated an enhancement in the heat transfer rate using a dovetail fin profile, followed by rectangular fin and trapezoidal fin profiles. Nabati et al. [15] utilized the Sinc collocation method to investigate the thermal performance of a porous fin subjected to a magnetic field and radiation. The accuracy of the proposed method was ensured through validation against the analytical and numerical approaches available in the literature.

Hoseinzadeh et al. [16] analysed heat transmission in a porous rectangular fin by applying various analytical techniques, including collocation, perturbation, and homotopy methods. The findings indicated an enhancement in heat transmission rate due to porosity, convection, and radiation parameters, with the radiation parameter exerting a significant impact on the overall temperature distribution.

Atouei et al. [17] examined the thermal performance of hemispherical fins by employing least square and collocation methods, considering temperature-dependent properties, heat generation, and radiation. Najafabadi et al. [18] investigated the heat dissipation between a cylindrical profile hot rod and its surroundings using radial basis function approximation.

Conventional coolants such as water and ethylene glycol, which are cost-effective and easily available, often struggle to effectively dissipate heat due to their lower thermal conductivity. This limitation can be mitigated by incorporating metallic nanoparticles that significantly enhance the fluid's thermal conductivity. Aravind and Ravikumar [19] analyzed the three-dimensional flow of rotating fluid over an infinite vertical oscillating plate by considering the fluid to be viscous, incompressible and electrically conducting. The results indicated an enhancement in the concentration as the chemical reaction parameter decreases and a decrease in the temperature due to high thermal radiation. Baslem et al. [20] investigated the thermal performance of a porous fin with three different types of water-based nanofluids. The research emphasized heat dissipation and concluded that it improves with an optimal balance between the nanofluid properties and the characteristics of the fin under wetted conditions.

Although the application of nanofluids improved thermal conductivity, limitations were observed in their rheological properties. These limitations were addressed by researchers incorporating two different nanoparticles in the base fluid. Goud et al. [21] investigated the heat transmission characteristics of a wetted dovetail fin immersed in ZnFe_2O_4 , $\text{MnZnFe}_2\text{O}_4$, and $\text{NiZnFe}_2\text{O}_4$ ternary combination of hybrid nanoparticles in a water-based fluid. The governing equations were solved numerically and analytically using the RKF method and DTM-Padé approximation. The findings revealed an enhanced thermal performance compared to hybrid nanofluid. Thermophysical characterization of Cu-graphene hybrid nanofluid was experimentally conducted by Shaik et al. [22]. At minimal concentration, the hybrid nanofluid showed an exceptional rise in thermal conductivity of 38% along with viscosity. Pai et al. [23] numerically investigated the thermal performance of a porous longitudinal rectangular

fin wetted with ternary hybrid nanofluid. Keerthi et al. [24] carried out an investigation into the thermal efficiency of a wet porous radial fin embedded in hybrid nanofluid using the RKF numerical technique. The results showed an enhancement in thermal efficiency with the rise in the volume fraction of nanoparticles. Hosseinzadeh et al. [25] carried out thermal analysis and experimentally validated a triplex tube heat exchanger equipped with tree-like fins, utilizing hybrid nanofluid containing MoS_2 and TiO_2 nanoparticles.

Pai et al. [26] numerically investigated the thermal performance of a hemispherical fin embedded in a hybrid nanofluid of various shapes. Hussain et al. [27] analysed the heat transmission rate of an exponential profile cylinder. A numerical investigation of nanofluid considering the transfer of mass and energy over a stretching and shrinking wedge was conducted by Alharbi et al. [28]. The results showed a boost in thermal efficiency, velocity, and the rate of mass transition. A study conducted by Din et al. [29] showed a notable impact of thermodynamic geometries on the thermal performance of the fin. Handique et al. [30] investigated the heat transfer behaviour of copper-water based hybrid nanofluids with various combinations of nanoparticles. The governing equations were non-dimensionalized and numerically solved using a Fortran algorithm. The results showed an enhancement in the heat transfer rate and mass transfer rate for Al_2O_3 -Cu-water combination at higher porosity parameter values. Alkasasbeh et al. [31] numerically analysed the heat transfer flow of TiO_2 , Al_2O_3 and GO nanoparticles in water and kerosene oil base fluids. The results showed that the Al_2O_3 -based nanofluid local wall temperature is higher compared to the rest of the nanofluids, whereas the skin friction of GO is more compared to the rest of the oxide nanoparticles. Numerical analysis on the heat and the mass transfer of the blood flow in the stenosed artery using a finite difference approach was conducted by Shankar and Siva [32]. The results showed a disorder in the blood velocity profile near the cholesterol deposition area at higher values of the Reynolds number. Mahalakshmi and Vennila et al. [33] numerically analysed the flow of nanofluid over a stretched exponential surface using the homotopy perturbation technique. Pai et al. [34] investigated the flow behaviour of a heat sink embedded in a binary combination of Al_2O_3 -SiC nanoparticles dispersed in a base fluid, with the objective of analyzing the impact of various similarity parameters on the heat transfer performance of the fin under convective and insulated tip boundary conditions. The results showed that the convective fin tip achieved an average heat transfer enhancement of 17.13% compared to the insulated fin tip.

Despite significant advancements in nanofluid based cooling systems, gaps remain in understanding the impact of various parameters on the overall thermal performance of the system. Although previous studies have explored the implications of using nanofluids and various fin profiles, the impact of expansion and contraction in the fin structure embedded in nanofluid has not been thoroughly investigated. The proposed model bridges these gaps by employing a novel technique, providing valuable insights into the impact of fin expansion and contraction on the temperature profile of the integrated system. In our present investigation, fin embedded in Fe_3O_4 - SiC - Al_2O_3 /Silicone oil ternary hybrid nanofluid is subjected to expansion and compression.

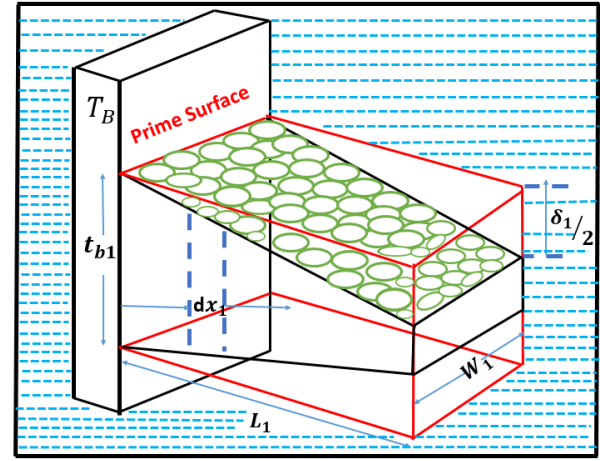


Fig. 1: Proposed model flow configuration

All three nanoparticles assist the base fluid to efficiently regulate the heat within the fin structure, due to their very high thermal conductivity. Traditional base fluids, such as water and ethylene glycol have been replaced by silicone oil in our study, due to its application at high operating temperatures. Also, its exceptional stability under variable temperature conditions makes it an excellent replacement for traditional base fluid in hybrid nanofluids [35]. Fe_3O_4 nanoparticle exhibits supermagnetic properties that help in enhancing the thermal efficiency in thermal management systems. Certain properties of SiC and Al_2O_3 nanoparticles, such as stability and resistance to corrosion, enable their use in harsh environments. Silicon carbide, due to its light weight and wide bandgap, finds applications in high power electronic devices, aerospace and automotive industries. The aim of our study is to characterise and analyse the fin temperature by analysing the variation in the structure for various similarity parameters using numerical technique.

II. MATHEMATICAL FORMULATION

Consider an axially aligned trapezoidal porous moving fin subjected to compression and expansion, embedded in Fe_3O_4 - SiC - Al_2O_3 / Silicone oil ternary hybrid nanofluid of volume fraction $\psi_1 = \psi_2 = \psi_3 = 0.01$. The proposed model arrangement is depicted in Fig. 1. Initially, the fin is considered stationary, with base temperature T_B and ambient temperature T_A , respectively. Subsequently, the fin experiences convection and radiation heat loss to the surrounding as it moves at a constant velocity. The fin is constructed using a homogeneous material, ensuring consistent thermal properties throughout the structure. Heat transfer within the fin occurs predominantly in one dimension along its length. The fin and the surrounding ternary hybrid nanofluid are in thermal equilibrium, ensuring a balanced heat exchange between the two.

$$\begin{aligned} Q(x_1 + dx_1) - Q(x_1) - A_1(x_1)h_1(T)(1 - \phi_1)(T - T_A)dx_1 \\ - h_{D1}i_{fg}A_1(x_1)(1 - \phi_1)(\hat{\omega} - \hat{\omega}_a) \\ - \sigma_1\epsilon_1A_1(x_1)dx_1(T^4 - T_A^4) - \dot{m}C_p(T - T_A) \\ + \rho C_p A_c(x_1)(1 + \hat{S}x_1)dx_1U_1 \frac{dT}{dx_1} = 0 \end{aligned} \quad (1)$$

The thermodynamic balance equation for an elemental length of an axially aligned fin under the pre-assumptions mentioned above is given by: Where the first and second term represent the heat transmission due to conduction, and the succeeding terms represent heat transmission due to convection. The area of cross-section at a distance x_1 is

$$A_c(x_1) = w_1 t(x_1),$$

where $t(x_1)$ represents the trapezoidal cross-section thickness, given by

$$t_{b1} - \delta_1 \left(1 - \frac{x_1}{L_1}\right).$$

The heat flux $Q(x_1)$ using Fourier's law of conduction is given by

$$Q(x_1) = A_c(x_1) k_{thnf} \cdot \frac{dT}{dx_1} \quad (2)$$

The heat transfer coefficient $h_1(T)$ is given by

$$h_1(T) = h_{a1} \frac{[T - T_A]^q}{[T_B - T_A]^q} = h_{D1} C_p (Le)^{2/3} \quad (3)$$

From Darcy's law, the mass flow rate of ternary hybrid nanofluid with density is given by

$$\dot{m} = (\rho_1)_{thnf} dx_1 \vartheta(x_1) P_1(x_1) \quad (4)$$

The flow velocity is defined as

$$\vartheta(x_1) = \frac{g_1 K_1 \beta_{thnf} (T - T_A)}{v_{thnf}} \quad (5)$$

The physical properties of nanofluid, hybrid nanofluid, and ternary hybrid nanofluid are detailed in Tables (I),(II) and (III).The table (IV) outlines the properties of each content of the ternary nanofluids.

TABLE I: PHYSICAL CHARACTERISTICS OF NANOFLUID

Thermal Conductivity	$k_{nf} = \frac{k_f(k_{p1} + (\alpha_1 - 1)k_f)}{(k_{p1} + (\alpha_1 - 1)k_f) + \varphi_1(k_f - k_{p1})} - \frac{(\alpha_1 - 1)\varphi_1 k_f(k_f - k_{p1})}{(k_{p1} + (\alpha_1 - 1)k_f) + \varphi_1(k_f - k_{p1})}$
Viscosity	$\vartheta_{nf} = \frac{\vartheta_f}{(1 - \varphi_1)^{2.5}}$
Coefficient of Thermal Expansion	$(\rho\beta)_{nf} = \varphi_1(\rho\beta)_{p1} + (1 - \varphi_1)(\rho\beta)_f$
Density	$(\rho_1)_{nf} = \varphi_1(\rho_1)_{p1} + (1 - \varphi_1)(\rho_1)_f$
Heat Capacity	$(\rho_1 C_p)_{nf} = \varphi_1(\rho_1 C_p)_{p1} + (1 - \varphi_1)(\rho_1 C_p)_f$

TABLE II: PHYSICAL CHARACTERISTICS OF HYBRID NANOFLUID

Thermal Conductivity	$k_{hnf} = \frac{k_{nf}(k_{p2} + (\alpha_1 - 1)k_{nf})}{(k_{p2} + (\alpha_1 - 1)k_{nf}) + \varphi_2(k_{nf} - k_{p2})} - \frac{(\alpha_1 - 1)k_{nf}\varphi_2(k_{nf} - k_{p2})}{(k_{p2} + (\alpha_1 - 1)k_{nf}) + \varphi_2(k_{nf} - k_{p2})}$
Viscosity	$\vartheta_{hnf} = \frac{\vartheta_f}{[(1 - \varphi_2)(1 - \varphi_1)]^{2.5}}$
Coefficient of Thermal Expansion	$(\rho\beta)_{hnf} = (1 - \varphi_1)(1 - \varphi_2)(\rho\beta)_f + \varphi_1(1 - \varphi_2)(\rho\beta)_{p1} + \varphi_2(\rho\beta)_{p2}$
Density	$\rho_{hnf} = (1 - \varphi_1)(1 - \varphi_2)\rho_f + \varphi_1(1 - \varphi_2)\rho_{p1} + \varphi_2\rho_{p2}$
Heat Capacity	$(\rho C_p)_{hnf} = (1 - \varphi_1)(1 - \varphi_2)(\rho C_p)_f + \varphi_1(1 - \varphi_2)(\rho C_p)_{p1} + \varphi_2(\rho C_p)_{p2}$

TABLE III: PHYSICAL CHARACTERISTICS OF TERNARY HYBRID NANOFLUID

Thermal Conductivity	$k_{thnf} = \frac{k_{nf}(k_{p3} + (\alpha_1 - 1)k_{nf})}{(k_{p3} + (\alpha_1 - 1)k_{nf}) + \varphi_3(k_{nf} - k_{p3})} - \frac{(\alpha_1 - 1)k_{nf}\varphi_3(k_{nf} - k_{p3})}{(k_{p3} + (\alpha_1 - 1)k_{nf}) + \varphi_3(k_{nf} - k_{p3})}$
Viscosity	$\vartheta_{thnf} = \frac{\vartheta_f}{[(1 - \varphi_2)(1 - \varphi_1)(1 - \varphi_3)]^{2.5}}$
Coefficient of Thermal Expansion	$(\rho\beta)_{thnf} = (1 - \varphi_1)(1 - \varphi_2)(1 - \varphi_3)(\rho\beta)_f + \varphi_1(1 - \varphi_2)(1 - \varphi_3)(\rho\beta)_{p1} + \varphi_3(\rho\beta)_{p3} + \varphi_2(1 - \varphi_3)(\rho\beta)_{p2}$
Density	$\rho_{thnf} = (1 - \varphi_1)(1 - \varphi_2)(1 - \varphi_3)\rho_f + \varphi_1(1 - \varphi_2)(1 - \varphi_3)\rho_{p1} + \varphi_2(1 - \varphi_3)\rho_{p2}$
Heat Capacity	$(\rho C_p)_{thnf} = \varphi_1(1 - \varphi_2)(1 - \varphi_3)(\rho C_p)_{p1} + \varphi_2(1 - \varphi_3)(\rho C_p)_{p2} + \varphi_3(\rho C_p)_{p3} + (1 - \varphi_1)(1 - \varphi_2)(1 - \varphi_3)(\rho C_p)_f$

TABLE IV: Properties of Each Content of the Fluids

Property	C_p (J/kgK)	ρ (kg/m ³)	β (1/K)	k (W/mK)
Silicone-oil	1460	960	94.5×10^{-5}	0.157
Fe ₃ O ₄	670	5180	1.3×10^{-5}	9.7
SiC	750	3210	0.277×10^{-5}	120
Al ₂ O ₃	440	8900	1.3×10^{-5}	91

The modified equation after substituting (2), (3), (4) and (5) in (1) is given as:

$$\begin{aligned} \frac{d}{dx_1} \left(k_{thnf} f(x_1) \frac{dT}{dx_1} \right) - 2h_1(T)(1 - \phi_1)(T - T_A) \\ - 2\sigma_1 \varepsilon_1 (T^4 - T_A^4) - 2h_{D1} i_{fg} (1 - \phi_1)(\hat{\omega} - \hat{\omega}_a) \\ + (\rho_1 C_p)_{tnnf} U_1 t(x_1) (1 + \hat{S} x_1) dx_1 \frac{dT}{dx_1} \\ - \frac{2(\rho_1 C_p)_{tnnf} g_1 K_1 (\rho_1 \beta)_{tnnf}}{v_{tnnf}} (T - T_A)^2 = 0 \end{aligned} \quad (6)$$

Since the fin tip is adiabatic, the boundary condition at the tip can be mathematically expressed as:

$$\begin{aligned} \frac{dT}{dx_1} &= 0, & \text{at } x_1 &= 0 \\ T &= T_B, & \text{at } x_1 &= L_1 \end{aligned} \quad (7)$$

On applying the dimensionless parameters to (6), we get

$$\begin{aligned} X &= \frac{x_1}{L_1}, & n_1 &= \frac{2h_{a1}(1 - \varphi_1) i_{fg} b_2 L_1^2}{k_f t_{b1} C_p (Le)^{2/3}}, \\ \Theta_1 &= \frac{T}{T_A}, & NC &= \frac{2(\rho_1 C_p)_f g_1 K_1 (\rho_1 \beta)_f T_B L_1^2}{\mu_f k_f t_{b1}}, \\ S_1 &= \hat{S} L_1, & PE &= \frac{(\rho_1 C_p)_f U_1 L_1}{k_f}, \\ A &= \frac{\delta_1}{t_{b1}}, & NR &= \frac{2\sigma_1 \varepsilon_1 T_B^3 L_1^2}{k_f t_{b1}}, \\ n_2 &= n_1 + n_0, & n_0 &= \frac{2h_{a1}(1 - \varphi_1) L_1^2}{k_f t_{b1}}, \\ \Theta_{1a} &= \frac{T_A}{T_B}, & (\bar{\omega} - \bar{\omega}_a) &= b_2(T - T_A). \end{aligned} \quad (8)$$

On substituting the (8) in (6) we get

$$\begin{aligned} (1 - A(1 - X)) \frac{d^2 \Theta_1}{dx^2} + A \frac{d\Theta_1}{dx} \\ + PE(1 + S_1 X) \frac{k_f}{k_{thnf}} \frac{(\rho_1 C_p)_{thnf}}{(\rho_1 C_p)_f} \frac{d\Theta_1}{dX} \\ - NC \frac{k_f}{k_{thnf}} \frac{(\rho_1 C_p)_{thnf}}{(\rho_1 C_p)_f} \frac{\partial f}{\partial thnf} \frac{(\rho_1 \beta)_{thnf}}{(\rho_1 \beta)_f} (\Theta_1 - \Theta_{1a})^2 \\ - NR \frac{k_f}{k_{thnf}} (\Theta_1^4 - \Theta_{1a}^4) - n_2 \frac{k_f}{k_{thnf}} \frac{(\Theta_1 - \Theta_{1a})^{q+1}}{(\Theta_1 - \Theta_{1a})^q} = 0 \end{aligned} \quad (9)$$

III. NUMERICAL SOLUTION

In this study, Lobatto numerical technique was employed to solve the derived nonlinear ordinary differential equation (ODE), due to its resilient stability and remarkable convergence properties. It offers superior accuracy compared to lower order methods such as Runge Kutta and Euler's method. Stiff ODEs, often encountered in heat transfer models can be handled using this technique. The approach divides the solution of differential equations into three interconnected stages. As each stage depends on the others, a balance is

maintained between accuracy and computational efficiency. The interdependence of the stages improves the method's ability to capture the intricate curvature of the solution, resulting in a precise representation of graphical outputs. The BVP4C function in MATLAB simulation tool incorporating Lobatto numerical technique was adopted to capture the thermal behaviour of the proposed model.

IV. RESULTS AND DISCUSSIONS

The interplay between the Fe₃O₄ - SiC - Al₂O₃ / Silicone oil ternary hybrid nanofluid and the porous structure of the fin is characterized by the wet porous parameter n_2 . Wet porous parameter significantly impacts the thermal performance of the fin under consideration by modulating the fluid retention. An increase in the porosity parameter enhances the fluid retention within the fin structure, leading to an increase in the effective heat capacity. This is due to the presence of additional fluid in the porous network that improves the thermal conduction and convective interactions. The impact of n_2 on the varying fin structure temperature distribution and temperature gradient are illustrated in Fig. 2 and 3. Our simulation results indicate an increase in the wet porous parameter results in progressive reduction in the fin temperature. Quantitatively, our simulation outcomes demonstrate a substantial improvement in the heat absorption due to fin contraction ($S_1 = -1$) from $S_1 = 0$ along its length. Specifically, for $n_2 = 0, 1$ and 2 , heat absorption improves by 1.71%, 1.81% and 1.83% respectively. The results suggest that an increase in the wet porous parameter along with the fin contraction promotes better heat dissipation, making the fin more thermally efficient.

The Fig. 4 and 5 illustrate the impact of NR on the temperature distribution and temperature gradient of the proposed fin under structural expansion and contraction. The simulation results indicate that an increase in the NR values decreases the thermal profile, while the temperature gradient increases. The variation suggests that the higher radiation level enhances the heat dissipation from the fin surface to the surrounding Fe₃O₄ - SiC - Al₂O₃ / Silicone oil ternary hybrid nanofluid, thereby improving the thermal transfer efficiency. The stronger radiative heat dissipation from the expanded fin surface results in greater energy exchange with the surrounding fluid, leading to improved cooling performance. Quantitatively, our simulation results indicate that the heat absorption improves by 1.818%, 1.824% and 1.831% as the fin undergoes contraction along its length corresponding to NR values of 1, 2, and 5 respectively. This suggests that an increase in NR values along with the fin contraction ($S_1 = -1$) from $S_1 = 0$ increases the heat absorption, thereby enhancing the overall thermal performance of the proposed model. In heat transfer studies, the strength of the convective heat transfer over the other thermal effects is characterized by the convective parameter NC . The impression of NC and S_1 parameters on the fin temperature distribution and temperature gradient are shown in Fig. 6 and 7. It is observed that an increase in the convective parameter for a given value of S_1 reduces the fin temperature and enhances the temperature gradient. This is due to the increased permeability effect, as the Darcy's number increases with higher NC values, easing the flow of fluid through the porous medium. The simulation outcome

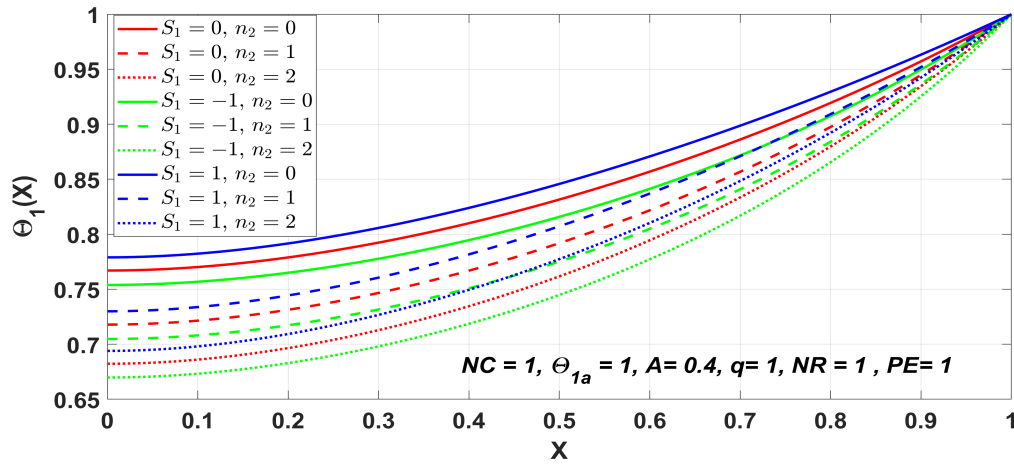


Fig. 2: Temperature characteristics of fin subjected to expansion and contraction under the influence of n_2 .

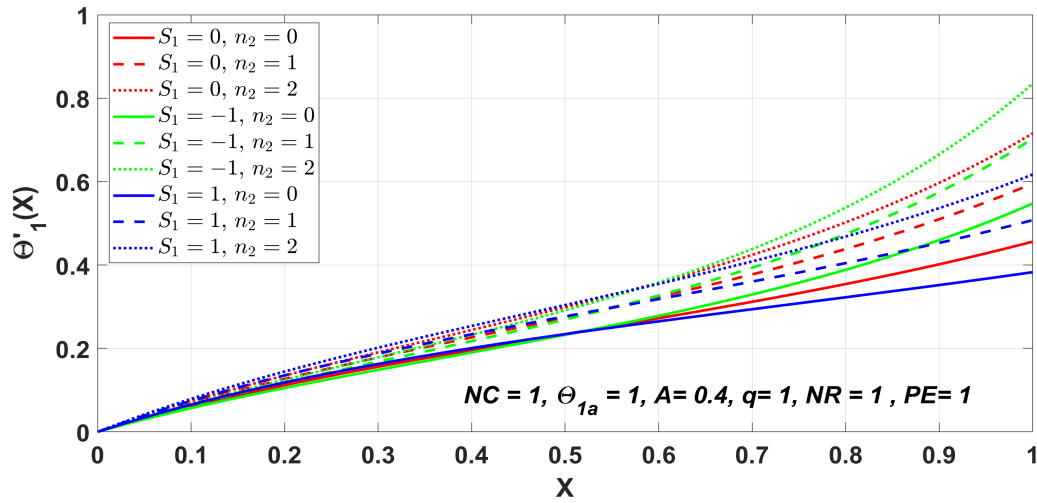


Fig. 3: Temperature gradient of fin subjected to expansion and contraction under the influence of n_2 .

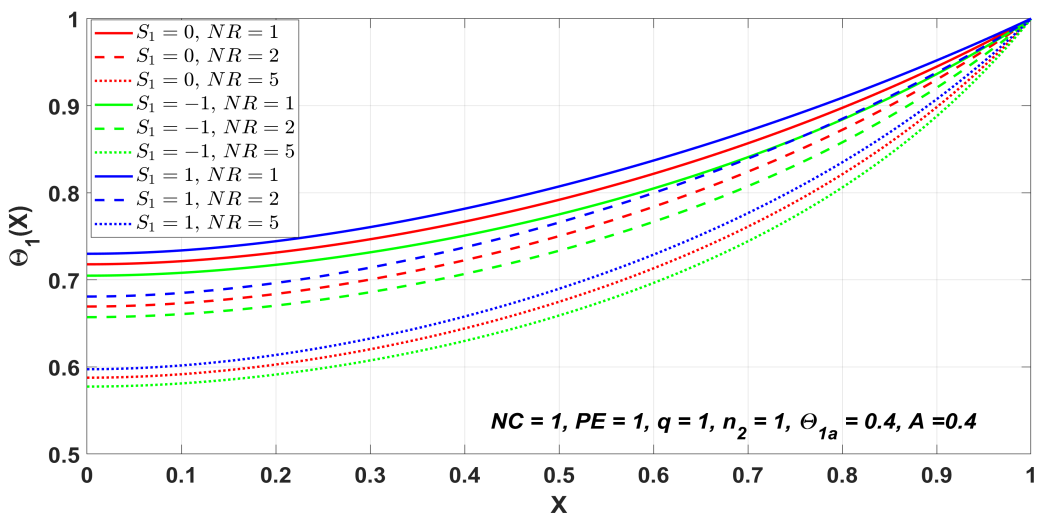


Fig. 4: Temperature characteristics of fin subjected to expansion and contraction under the influence of NR .

shows an enhancement in heat absorption by 1.81%, 1.83% and 1.84% with the fin contraction along its length from $S_1 = 0$ for $NC = 1, 2$, and 5 respectively. This trend

indicates that the enhanced convective effects along with the fin contraction ($S_1 = -1$) from $S_1 = 0$ increases the heat absorption, thereby improving the overall thermal

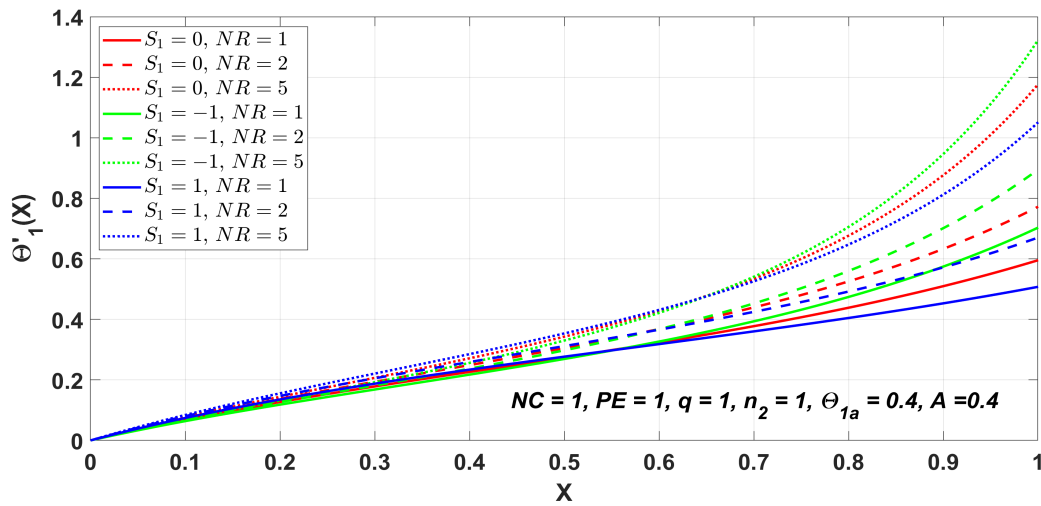


Fig. 5: Temperature gradient of fin subjected to expansion and contraction under the influence of NR .

performance of the proposed model. The convective to diffusive heat transport ratio parameter PE plays a key role in characterizing the heat transfer in heat exchangers. Its effect on the thermal distribution and thermal gradient along the fin length under structural expansion and contraction are shown in Fig. 8 and 9. For a given value of S_1 , an increase in the PE values lead to rise in the fin's thermal profile due to increased velocity of the fin at higher PE values, reducing its exposure time to the surrounding environment. Our simulation results indicate a progressive enhancement in the heat absorption by 1.82%, 3.26% and 5.11% as the fin undergoes contraction along its length, corresponding to PE values of 1, 2 and 4 respectively. This observation indicates greater thermal retention with an increase in PE values but also highlights the trade-off between heat accumulation and dissipation efficiency. The q parameter characterizes the flow behaviour of ternary hybrid nanofluid. Its influence on the contracting and expanding fin temperatures, as well as its temperature gradients, graphically illustrated in Fig. 10 and 11. An increment in the value of q parameter at a given value of S_1 enhances the fin temperature and reduces the thermal gradient. This occurs due to the greater resistance experienced by the fluid from the non-linearity in its flow, trapping the heat and maintaining the fin warmer. Conversely at the lower values of q parameter, the fluid flow remains linear, allowing the heat to dissipate more efficiently from the fin surface due to reduced resistance, keeping the fin cooler. The simulation outcome shows an enhancement in the heat absorption by 1.65%, 1.82% and 2.27% with the fin contraction along its length from $S_1 = 0$ for $q = 2, 1$ and 0 respectively. The effect of Θ_{1a} on the contracting and expanding fin temperatures, as well as its temperature gradients, are graphically demonstrated in Fig. 12 and 13. An increment in the values of ambient temperature at a given S_1 value enhances the fin temperature, indicating a reduction in the convective heat transfer due to the decrease in the thermal gradient between the fin and the surrounding ternary hybrid nanofluid. The simulation outcome shows an enhancement in the heat absorption by 0.60%, 1.82%, and 3.46% with the fin contraction along its length from $S_1 = 0$ for $\Theta_{1a} = 0.8, 0.4$, and 0 respectively. The taper ratio of the

fin plays a significant role in promoting the heat dissipation from the fin surface. The influence of this parameter on the thermal distribution and thermal gradient along the fin length under structural expansion and contraction are shown in Fig. 14 and 15. The simulation results indicate a dip in the thermal profile of the fin for both structural expansion and contraction, signifying an enhancement in the heat dissipation. The thermal gradient along the fin length increases with increasing A . This variation can be attributed to the expansion in the surface area resulting from an inclined fin profile, compared to a standard rectangular profile ($A = 0$). The greater surface area exposure enhances the convective interactions with the surrounding Fe_3O_4 - SiC - Al_2O_3 /Silicone oil ternary hybrid nanofluid, enhancing the heat transfer rate. Quantitatively, the heat absorption enhances by 2.02%, 3.03% and 3.22% with the fin contraction along its length from $S_1 = 0$ for $A = 0, 0.4$ and 0.8 respectively. The results highlight the importance of structural modifications in the heat exchanger design, where optimizing the taper ratio can improve the heat dissipation without the requirement of an additional cooling mechanism.

Fig. 16 illustrates the percentage improvement in heat transfer as a function of NC and S_1 under fixed thermal and flow conditions. The results reveal that an increase in the values of NC enhances the heat transfer across all surface contraction levels of S_1 , confirming the role of stronger convection in promoting efficient energy exchange within the porous medium. Conversely, as the surface contraction becomes more intense, i.e., as S_1 approaches -1 , the percentage improvement in heat transfer gradually declines, especially at higher NC values. This trend indicates that excessive contraction may suppress fluid mixing or reduce boundary layer thickness, thereby limiting the thermal advantage otherwise provided by hybrid nanoparticle dispersion. Overall, the interplay between convective strength and geometric deformation demonstrates that moderate contraction combined with enhanced convection delivers optimal heat transfer enhancement, particularly under the influence of quaternary nanofluids. Fig. 17 presents the variation in percentage enhancement of the temperature gradient as influenced by NC and S_1 . The results show a decreasing

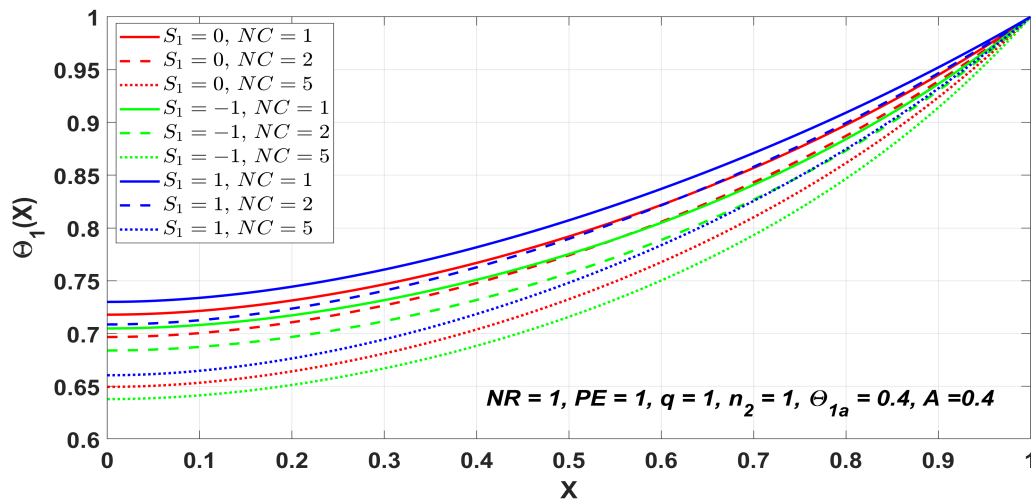


Fig. 6: Temperature characteristics of fin subjected to expansion and contraction under the influence of NC .

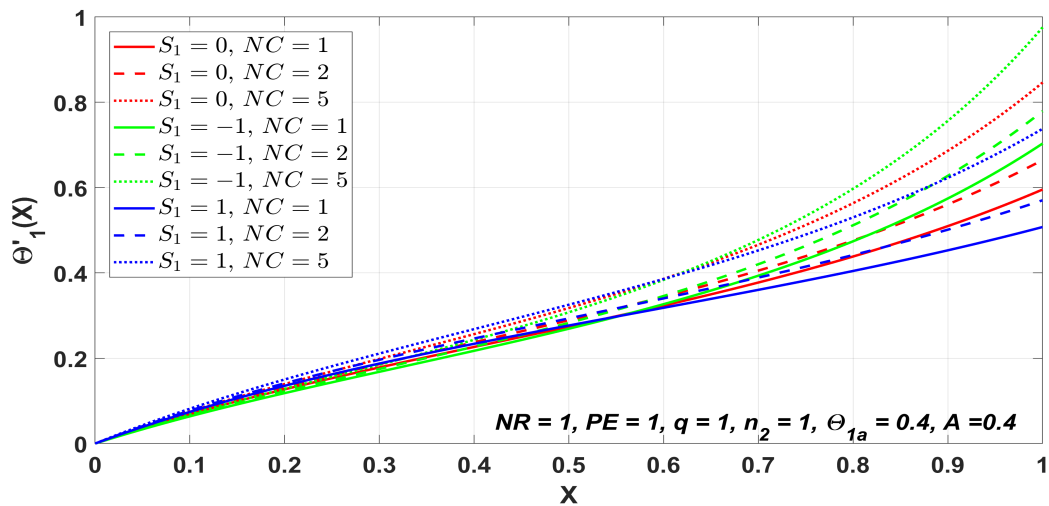


Fig. 7: Temperature gradient of fin subjected to expansion and contraction under the influence of NC .

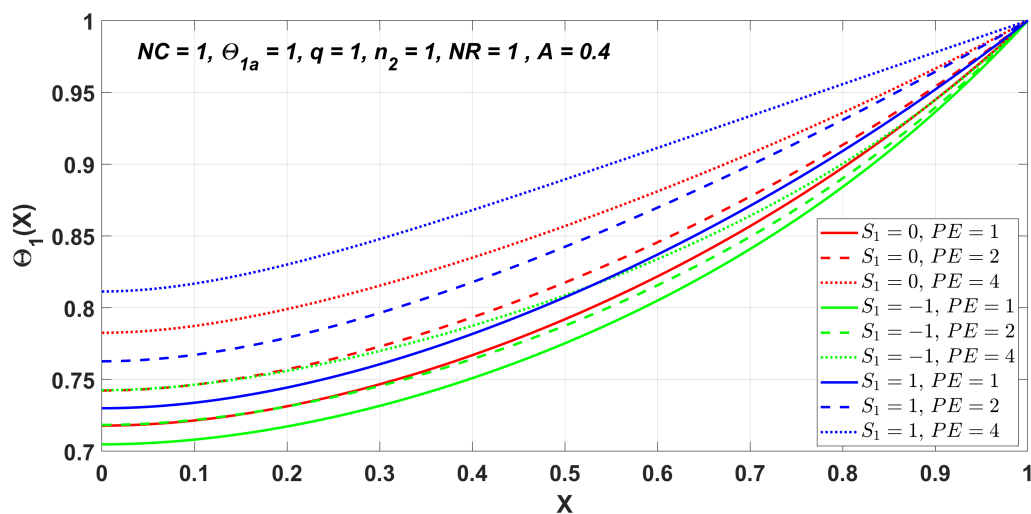


Fig. 8: Temperature characteristics of fin subjected to expansion and contraction under the influence of PE .

trend in temperature gradient enhancement with increasing NC values across all values of S_1 . This implies that as convection becomes more dominant, the axial temperature

difference within the fluid domain reduces, leading to a more uniform temperature profile and weaker thermal gradient near the surface. Additionally, stronger values of S_1 result in a

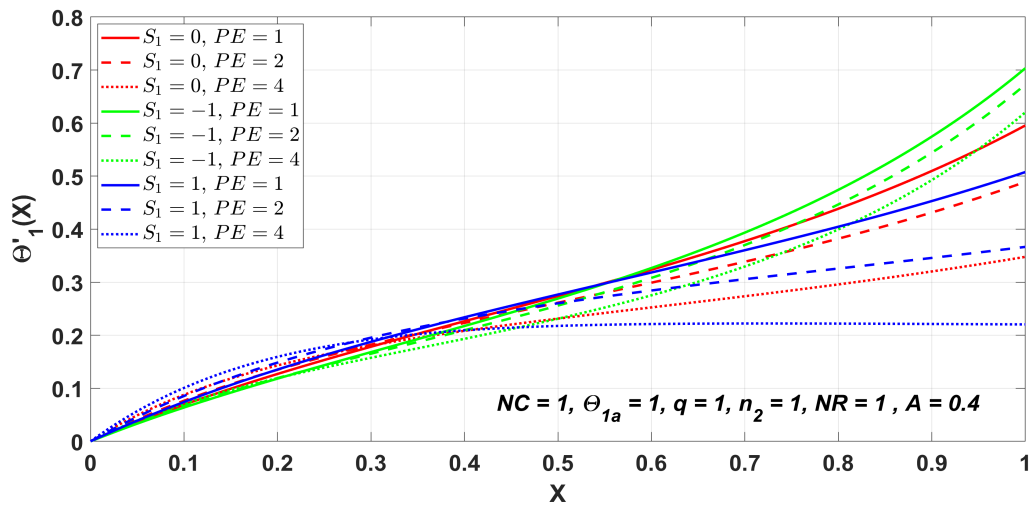


Fig. 9: Temperature gradient of fin subjected to expansion and contraction under the influence of PE .

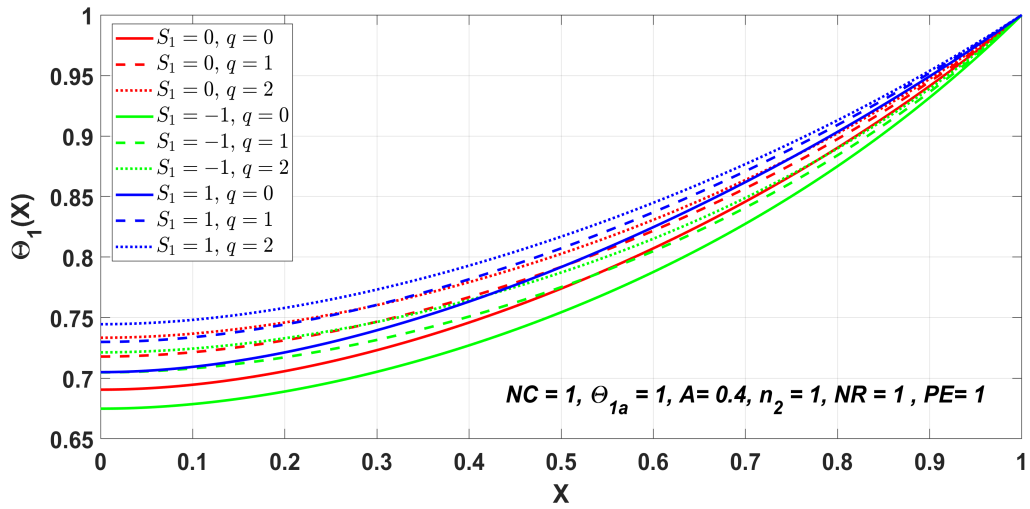


Fig. 10: Temperature characteristics of fin subjected to expansion and contraction under the influence of q .

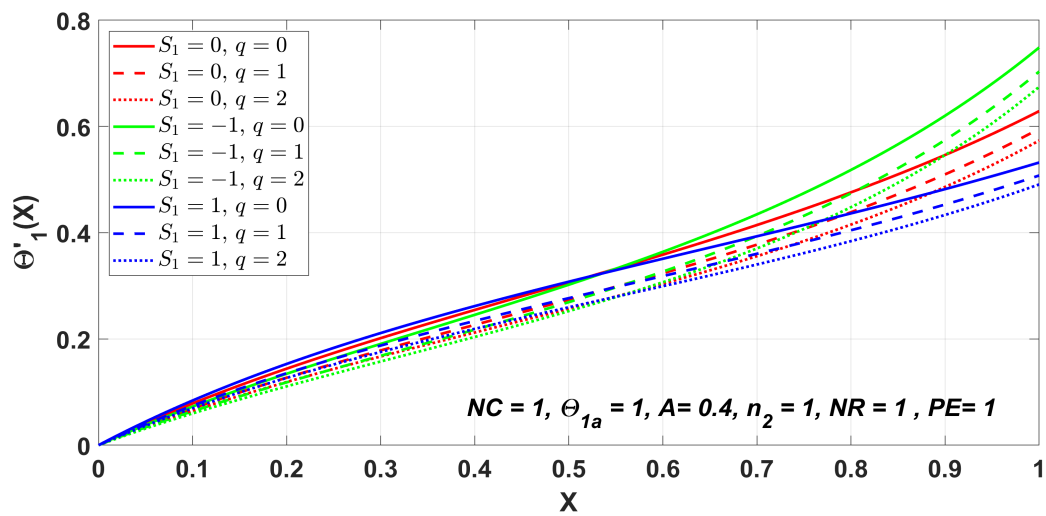


Fig. 11: Temperature gradient of fin subjected to expansion and contraction under the influence of q

steeper decline in the enhancement percentage, indicating that contraction suppresses the development of the thermal boundary layer. This behaviour suggests that while higher

NC may aid in heat removal, it comes at the cost of a reduced local temperature gradient, which could be critical in applications requiring steep thermal differentials, such as

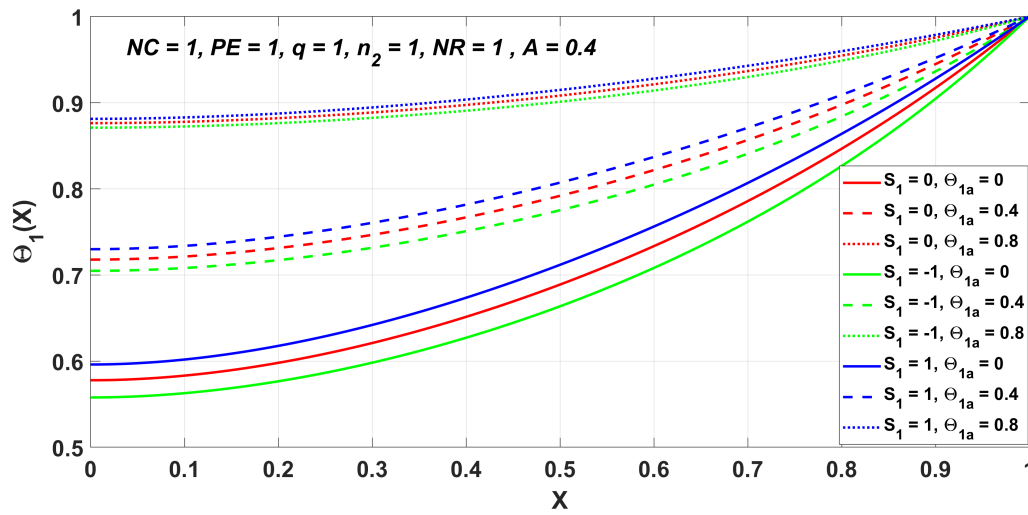


Fig. 12: Temperature characteristics of fin subjected to expansion and contraction under the influence of θ_{1a} .

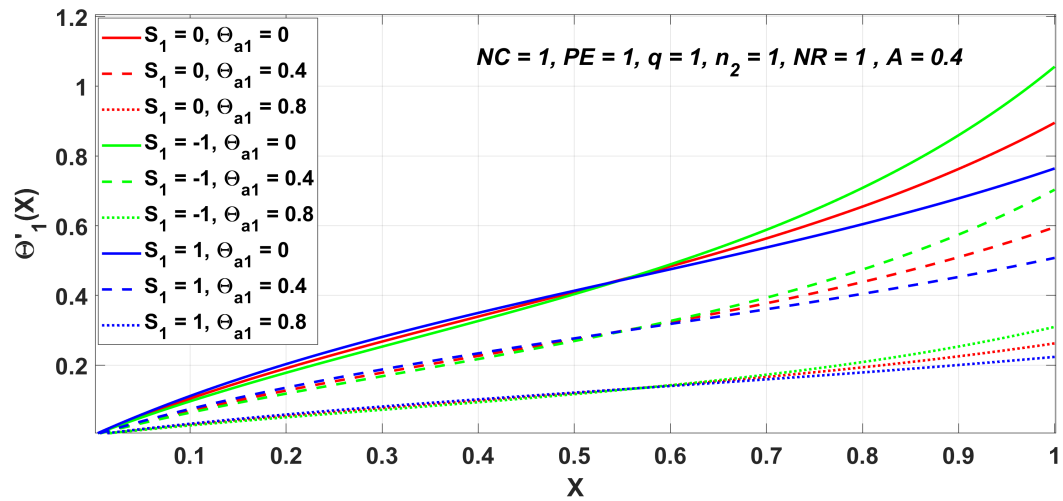


Fig. 13: Temperature gradient of fin subjected to expansion and contraction under the influence of θ_{1a}

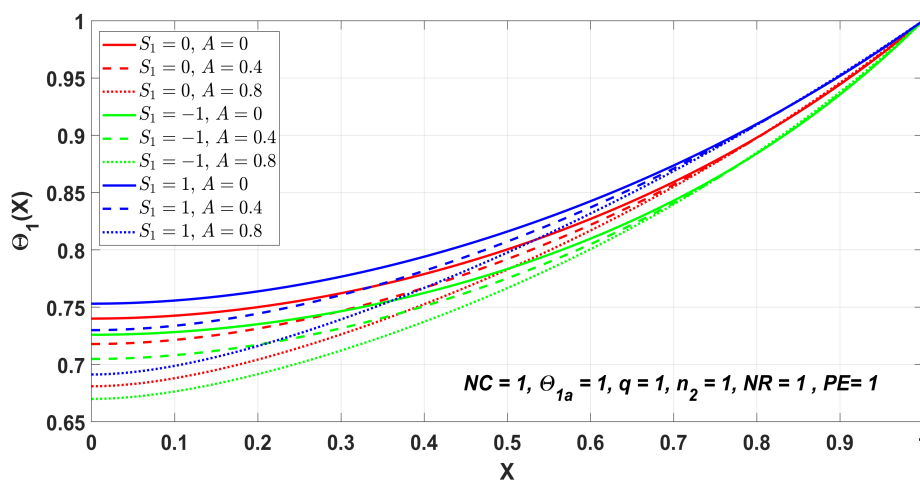


Fig. 14: Temperature characteristics of fin subjected to expansion and contraction under the influence of A

thermoelectric systems or high-precision thermal controls. Thus, a trade-off between heat transfer and thermal gradient must be considered to optimize the thermal performance of

nanoparticle-embedded wet porous heat sink systems.

Fig. 18 illustrates the variation in percentage improvement in heat transfer with respect to NR and S_1 values under fixed

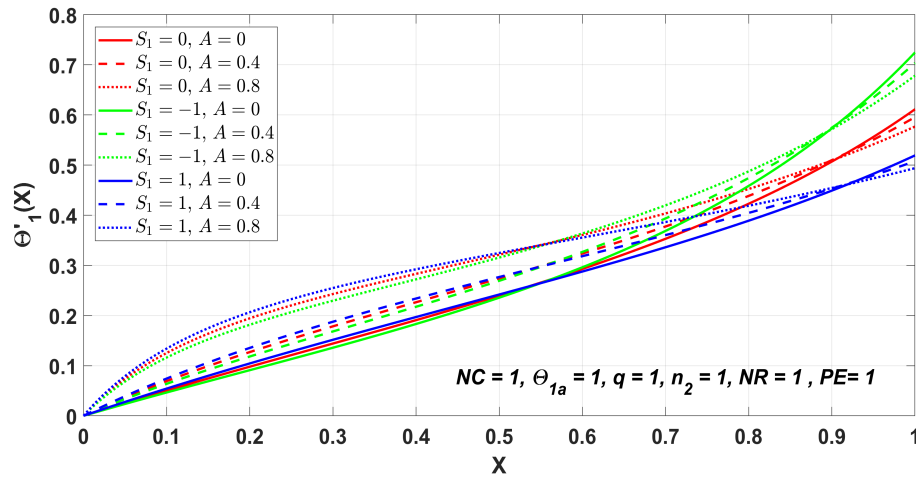


Fig. 15: Temperature gradient of fin subjected to expansion and contraction under the influence of A

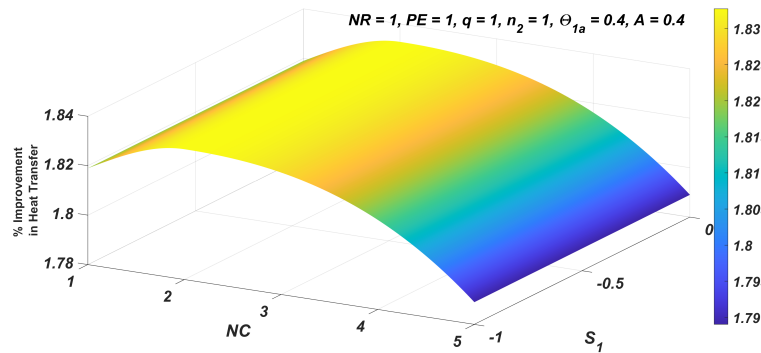


Fig. 16: Variation of % improvement in heat transfer as a function of NC and S_1

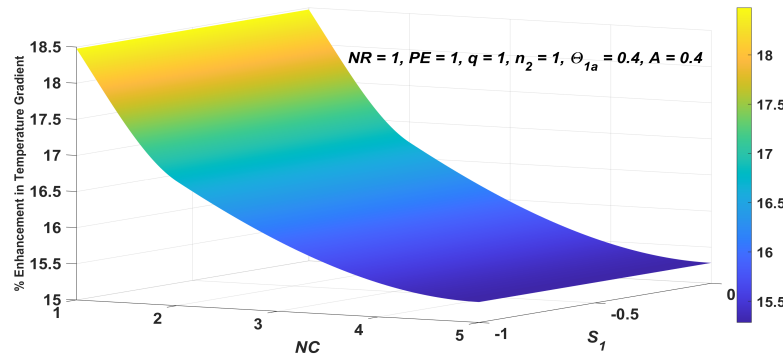


Fig. 17: Variation of % improvement in temperature gradient as a function of NC and S_1

thermal and flow conditions. The plot demonstrates that as the radiation parameter NR increases, the percentage improvement in heat transfer progressively decreases, implying a weakening influence of radiative effects on convection-driven heat transmission in the porous fin. Additionally, the plot shows that stronger contraction consistently results in better heat transfer performance at lower values of NR , highlighting the combined influence of geometric deformation and radiation effects, where surface contraction can enhance heat transfer and promote fluid mixing. The surface plot shown in Fig. 19 indicates a noticeable decline in temperature gradient as NR increases. This behaviour

highlights the attenuating effect of thermal radiation, which tends to make the temperature more uniform and reduces the temperature difference across the porous fin. Furthermore, as the surface contracts more, the temperature gradient becomes even smaller, especially when the radiation is high (i.e., at higher values of NR). This suggests that the combined effect of geometric contraction and stronger radiation can limit the temperature gradient, which could negatively impact the thermal performance of systems relying on steep thermal gradients, such as in energy harvesting applications. Thus, for optimal thermal system design, a balanced tuning of contraction and radiative parameters is essential.

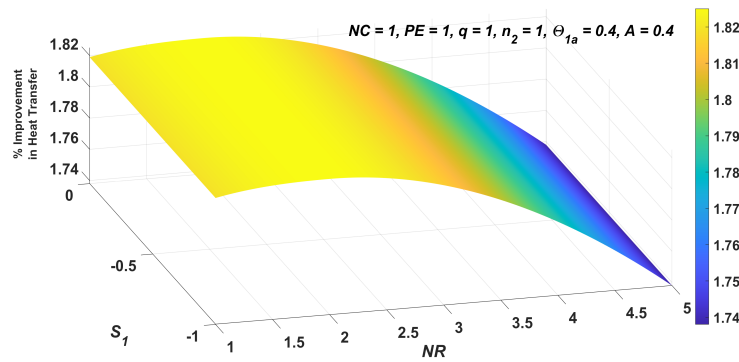


Fig. 18: Variation of % improvement in heat transfer as a function of NR and S_1

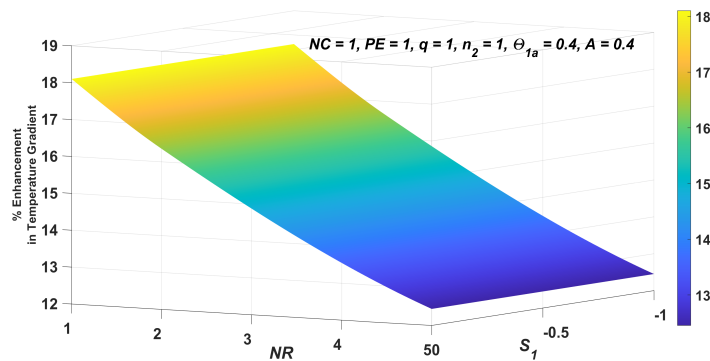


Fig. 19: Variation of % improvement in temperature gradient as a function of NR and S_1

V. CONCLUSION

The numerical investigation of our proposed model demonstrates the potential impact of fin contraction embedded in a ternary hybrid nanofluid on the heat transfer. The following conclusions were drawn on a moving fin subjected to contraction, with the variations in the *similarity* parameters.

- The heat absorption increases with the fin contraction and rise in the values of wet porous, convective, and radiative parameters.
- The heat absorption increases with the fin contraction and decrease in the values of Peclet number, exponential index, and ambient temperature.
- The thermal gradient increases with the fin contraction and rise in the values of wet porous, convective, and radiative parameters.
- The thermal gradient increases with the fin contraction and decrease in the Peclet number, exponential index, and ambient temperature.

The fin temperature increases with the transition in the fin structure from contraction to expansion, while the thermal gradient decreases. The variation can be effectively utilized for faster heat transmission during accumulation of thermal energy on the surface. Hence, the distribution of temperature over the fin can be maintained by optimizing the S_1 parameter.

REFERENCES

- [1] M. Benkhedda, T. Boufendi, T. Tayebi, and A. J. Chamkha, "Convective heat transfer performance of hybrid nanofluid in a horizontal pipe considering nanoparticles shapes effect," *Journal of Thermal Analysis and Calorimetry*, vol. 140, no. 1, pp. 411-425, 2020.
- [2] M. Farhan, M. Saad Hameed, H. M. Suleman, and M. Anwar, "Heat transfer enhancement in transformers by optimizing fin designs and using nanofluids," *Arabian Journal for Science and Engineering*, vol. 44, no. 6, pp. 5733-5742, 2019.
- [3] F. Ma, T. Zhu, Y. Zhang, X. Lu, W. Zhang, and F. Ma, "A review on heat transfer enhancement of phase change materials using fin tubes," *Energies*, vol. 16, no. 1, p. 545, 2023.
- [4] A. Gaikwad, A. Sathe, and S. Sanap, "A design approach for thermal enhancement in heat sinks using different types of fins: A review," *Frontiers in Thermal Engineering*, vol. 2, p. 980985, 2023.
- [5] O. Sharma, S. D. Barewar, and S. S. Chougule, "Experimental investigation of heat transfer enhancement in pool boiling using novel Ag/ZnO hybrid nanofluids," *Journal of Thermal Analysis and Calorimetry*, vol. 143, pp. 1051-1061, 2021.
- [6] A. R. Dhumal, A. P. Kulkarni, and N. H. Ambhore, "A comprehensive review on thermal management of electronic devices," *Journal of Engineering and Applied Science*, vol. 70, no. 1, p. 140, 2023.
- [7] C. Kannan, P. Sathyabalan, and S. Ramanathan, "A numerical research of heat transfer in rectangular fins with different perforations," *International Journal of Innovative Technology and Exploring Engineering*, vol. 8, no. 12S, pp. 367-371, 2019.
- [8] A. M. Abdulateef, S. Mat, J. Abdulateef, K. Sopian, and A. A. Al-Abidi, "Geometric and design parameters of fins employed for enhancing thermal energy storage systems: a review," *Renewable and Sustainable Energy Reviews*, vol. 82, pp. 1620-1635, 2018.
- [9] D. S. Khudhur, R. C. Al-Zuhairi, and M. S. Kassim, "Thermal analysis of heat transfer with different fin geometry through straight plate-fin heat sinks," *International Journal of Thermal Sciences*, vol. 174, p. 107443, 2022.
- [10] B. Kundu and S. Wongwises, "A decomposition analysis on convecting-radiating rectangular plate fins for variable thermal conductivity and heat transfer coefficient," *Journal of the Franklin Institute*, vol. 349, no. 3, pp. 966-984, 2012.
- [11] G. K. Ramesh, G. R. Manohar, J. K. Madhukesh, P. Venkatesh, and B. J. Gireesha, "Thermal aspects of a radiative-convective semi-spherical porous fin of functionally graded material," *The European Physical Journal Plus*, vol. 139, no. 1, p. 97, 2024.
- [12] H. Asadian, M. Zaretabar, D. D. Ganji, M. Gorji-Bandpy, and S. Sohrabi, "Investigation of heat transfer in rectangular porous

- fins (Si_3N_4) with temperature-dependent internal heat generation by Galerkin's method (GM) and Akbari-Ganji's method (AGM)," International Journal of Applied and Computational Mathematics, vol. 3, pp. 2987-3000, 2017.
- [13] M. T. Darvishi, R. S. R. Gorla, and F. Khani, "Natural convection and radiation in porous fins," International Journal of Numerical Methods for Heat & Fluid Flow, vol. 23, no. 8, pp. 1406-1420, 2013.
- [14] N. A. Khan, M. Sulaiman, and F. S. Alshammari, "Heat transfer analysis of an inclined longitudinal porous fin of trapezoidal, rectangular, and dovetail profiles using cascade neural networks," Structural and Multidisciplinary Optimization, vol. 65, no. 9, p. 251, 2022.
- [15] M. Nabati, M. Jalalvand, and S. Taherifar, "Sinc collocation approach through thermal analysis of porous fin with magnetic field," Journal of Thermal Analysis and Calorimetry, vol. 144, pp. 2145-2158, 2021.
- [16] S. Hoseinzadeh, P. S. Heyns, A. J. Chamkha, and A. Shirkhani, "Thermal analysis of porous fins enclosure with the comparison of analytical and numerical methods," Journal of Thermal Analysis and Calorimetry, vol. 138, pp. 727-735, 2019.
- [17] S. A. Atouei, K. Hosseinzadeh, M. Hatami, S. E. Ghasemi, S. A. R. Sahebi, and D. D. Ganji, "Heat transfer study on convective-radiative semi-spherical fins with temperature-dependent properties and heat generation using efficient computational methods," Applied Thermal Engineering, vol. 89, pp. 299-305, 2015.
- [18] M. F. Najafabadi, H. T. Rostami, K. Hosseinzadeh, and D. D. Ganji, "Thermal analysis of a moving fin using the radial basis function approximation," Heat Transfer, vol. 50, no. 8, pp. 7553-7567, 2021.
- [19] A. A. G. Aravind and J. Ravikumar, "Effects of thermal radiation in a rotating fluid on an oscillating vertical plate with variable temperature and mass diffusion," IAENG International Journal of Applied Mathematics, vol. 54, no. 1, pp. 128-139, 2024.
- [20] A. Baslem, G. Sowmya, B. J. Gireesha, B. C. Prasannakumara, M. Rahimi-Gorji, and N. M. Hoang, "Analysis of thermal behavior of a porous fin fully wetted with nanofluids: convection and radiation," Journal of Molecular Liquids, vol. 307, p. 112920, 2020.
- [21] J. S. Goud, P. Srilatha, R. S. V. Kumar, K. T. Kumar, U. Khan, Z. Raizah, H. S. Gill, and A. M. Galal, "Role of ternary hybrid nanofluid in the thermal distribution of a dovetail fin with the internal generation of heat," Case Studies in Thermal Engineering, vol. 35, p. 102113, 2022.
- [22] A. H. Shaik, S. Chakraborty, S. Saboor, K. R. Kumar, A. Majumdar, M. Rizwan, and M. R. Chandan, "Cu-graphene water-based hybrid nanofluids: synthesis, stability, thermophysical characterization, and figure of merit analysis," Journal of Thermal Analysis and Calorimetry, vol. 149, no. 7, pp. 2953-2968, 2024.
- [23] A. G. Pai and R. G. Pai, "Thermal characterization of porous longitudinal rectangular moving fin wetted with $\text{GO-MoS}_2\text{-Al}_2\text{O}_3/\text{C}_2\text{H}_6\text{O}_2\text{-H}_2\text{O}$ ternary hybrid nanofluid," Cogent Engineering, vol. 11, no. 1, p. 2364052, 2024.
- [24] M. L. Keerthi, B. J. Gireesha, and G. Sowmya, "Numerical investigation of efficiency of fully wet porous convective-radiative moving radial fin in the presence of shape-dependent hybrid nanofluid," International Communications in Heat and Mass Transfer, vol. 138, p. 106341, 2022.
- [25] K. Hosseinzadeh, A. R. Mogharrebi, A. Asadi, M. Paikar, and D. D. Ganji, "Effect of fin and hybrid nanoparticles on solid process in hexagonal triplex latent heat thermal energy storage system," Journal of Molecular Liquids, vol. 300, p. 112347, 2020.
- [26] A. G. Pai, R. G. Pai, K. Pradeep, and L. Raj, "Dynamic characterization and optimization of heat flux and thermal efficiency of a penetrable moving hemispherical fin embedded in a shape optimized $\text{Fe}_3\text{O}_4\text{-Ni/C}_6\text{H}_{18}\text{OSi}_2$ hybrid nanofluid: L-III A solution," Symmetry, vol. 16, no. 11, p. 1532, 2024.
- [27] F. Hussain, A. Hussain, and S. Nadeem, "Unsteady shear-thinning behaviour of nanofluid flow over exponential stretching/shrinking cylinder," Journal of Molecular Liquids, vol. 345, p. 117894, 2022.
- [28] K. A. M. Alharbi, M. Bilal, R. Allogmany, and A. A. Ali, "The numerical study of nanofluid flow with energy and mass transfer over a stretching/shrinking wedge," Proceedings of the Institution of Mechanical Engineers, Part E: Journal of Process Mechanical Engineering, vol. 237, no. 6, pp. 2134-2143, 2023.
- [29] Z. U. Din, A. Ali, Z. A. Khan, and G. Zaman, "Heat transfer analysis: convective-radiative moving exponential porous fins with internal heat generation," Mathematical Biosciences and Engineering, vol. 19, no. 11, pp. 11491-11511, 2022.
- [30] P. Handique, P. S. Doley, S. Maity, A. V. Kumar, and L. Jino, "MHD double-diffusive convection flow of hybrid nanofluid over the vertical plate under porous medium," Engineering Letters, vol. 32, no. 9, pp. 1728-1749, 2024.
- [31] H. T. Alkasasbeh, M. Z. Swalmeh, A. Hussanan, and M. Mamat, "Numerical solution of heat transfer flow in micropolar nanofluids with oxide nanoparticles in water and kerosene oil about a horizontal circular cylinder," IAENG International Journal of Applied Mathematics, vol. 49, no. 3, pp. 326-333, 2019.
- [32] G. Shankar and E. P. Siva, "A numerical investigation of thermal and mass exchange of blood along porous stenosis arterial flow with applied magnetic field," IAENG International Journal of Applied Mathematics, vol. 54, no. 3, pp. 532-541, 2024.
- [33] D. Mahalakshmi and B. Vennila, "Computational investigation on flow of nanofluid past an exponentially stretching surface using VHPM," IAENG International Journal of Applied Mathematics, vol. 54, no. 5, pp. 902-909, 2024.
- [34] A. G. Pai, R. G. Pai, A. A. Samat, and A. B. Laxmish, "Numerical modelling and optimization of thermal performance of heat sink with uniform cross-sectional area using shape optimized $\text{Al}_2\text{O}_3\text{-SiC}$ nanoparticles in base fluid," Journal of Advanced Research in Fluid Mechanics and Thermal Sciences, vol. 125, no. 2, pp. 145-169, 2025.
- [35] A. Arifuzzaman, R. Saidur, and N. Aslfattahi, "MXene and functionalized graphene hybridized nanoflakes-based silicone-oil nanofluids as a new class of media for micro-cooling application," Ceramics International, vol. 49, no. 4, pp. 5922-5935, 2023.